Tellus (1997), 49B, 300–313
Printed in UK – all rights reserved

TELLUS
ISSN 0280–6509

The number of sea-salt, sulfate, and carbonaceous particles in the marine atmosphere:

EM measurements consistent with the ambient size distribution

By LYNN MCINNES*, DAVID COVERT† and BRAD BAKER‡ **NOAA Climate Monitoring and Diagnostics Laboratory, R/E/CG1, 325 Broadway, Boulder CO 80303, USA; †Department of Atmospheric Sciences, University of Washington, Seattle WA 98195, USA; ‡Department of Chemistry, University of Colorado, Boulder CO 80309, USA.*

(Manuscript received 3 April 1996; in final form 8 January 1997)

ABSTRACT

To evaluate the number of sea-salt, sulfate, and carbonaceous particles associated with the fine and coarse mode aerosol in the marine boundary layer and from the marine/continental interface, the elemental composition of individual aerosol particles was determined with EM. Samples were collected from the Pacific marine boundary layer during a research cruise along 140°W from the southern to northern hemisphere, and from a coastal station in NW Washington. Consistently, the most dominant aerosol types found were ammonium sulfate and acidic sulfate comprising 52 to 96% of the total number at a median diameter of 0.14 μm. Sea-salt particles were 4 to 13% of the total number, with modes at 0.2 and 0.6 μm. Carbonaceous particles, mostly as organic compounds, made up the remainder of the submicrometer aerosol at a few % to as much as 31% of the total number for continentally influenced periods. Silica-rich minerals and potassium and calcium salts were observed during such periods, representing a measurable, but small fraction of the total number. Sea-salt particles were 86 to 100% of the number of supermicrometer particles with a mass median diameter of 1.5 μm. A less abundant, and variable fraction of mineral particles made up the remainder of the coarse aerosol number concentration identified primarily as aluminosilicates, mass median diameter of 0.9 μm. Very little soot was observed in either the coarse or fine mode. Particle number concentrations were consistently low and airmass trajectories suggest the air originated over the open ocean for the majority of the sampling periods. Overall, normalized EM distributions agreed fairly well with in-situ measurements of the aerosol size distribution.

1. Introduction

1.1. Techniques of individual particle analysis

The ambient aerosol consists of a distribution of chemical compositions with corresponding variations in aerosol physical properties (or behavior) as a function of aerosol size, and often with variations within a narrow size range (Covert and Heintzenberg, 1990). The presence of such mixtures in the aerosol population, often referred to as external mixtures, requires that the population is treated with respect to measurements and models as chemically distinct subsets, with their own unique properties. These can be used to identify sources and production processes and model subsequent chemical interactions, cloud formation, and removal processes. Measurements of mass-weighted concentrations by conventional techniques, masks the microscale variability in the aerosol composition which exists between particles, as a result of sources and atmospheric

* Corresponding author. Email: lmcinnes@cmdl.noaa.gov.

processing. Only individual particle analysis techniques can resolve differences in the size, chemical composition, and relative abundance of aerosol particles and put such information in the context of aerosol number and mass concentrations. Analytical techniques for individual particles include laser ionization mass spectrometry (Prather et al., 1994; Murphy and Thomson, 1995), laser microprobe mass analysis (Bruynseels and Van Greiken, 1984; Wouters et al., 1990; Dierck et al., 1992), analytical electron microscopy (Okada et al., 1990; Artaxo et al., 1992; Sheridan et al., 1992; Mouri and Okada, 1993; McInnes et al., 1994), in-situ flame photometric detection (Radke, 1968), and tandem differential mobility analysis of pre-conditioned aerosol particles (McMurry and Stolzenburg, 1989; Covert and Heintzenberg, 1993). Each technique offers its own particular advantages and limitations, and no one technique can independently determine the chemical composition and heterogeneity of the entire aerosol population, which extends from a few nanometers to tens of micrometers in size.

Laser ionization mass spectrometry can rapidly analyze ambient aerosol particles larger than 0.2 μm in diameter. The scattered light from a continuous He-Ne laser is used to estimate the particle size and trigger an excimer laser which ionizes the molecules in the particle. Ions are accelerated into a time of flight, TOF, mass spectrometer where individual particle spectra, containing elemental and molecular information, are collected. The instrument is able to identify trace constituents such as water clusters in the spectra (Murphy and Thomson, 1995). The technique can also identify individual particle mixtures of organic and inorganic material (Prather et al., 1994). Volatile species, such as nitric acid, are preserved, since the particles spend a short time, 0.5 ms, in the vacuum environment. The technique is currently most appropriate for qualitative identification of aerosol composition. Individual particle spectra are acquired in either the positive or negative ion mode. Low light scattering signals from small particles limit the lower-size resolution of the technique. Quantitative analysis has proven difficult because ion yields obtained from same sized laboratory particles are not reproducible.

Laser microprobe mass analysis (LAMMA) is an earlier technique utilizing a mass spectrometer, which is now used routinely for individual particle characterization. Aerosol particles are collected onto a substrate and mounted in the ionizing region of the instrument. The chemical composition of a particle is determined after evaporation with a Nd : YAG laser pulse. Atomic and molecular ions are formed and accelerated into the TOF mass spectrometer where information concerning the chemical composition of the particle is acquired. An optical microscope is used to determine the size and morphology of the particles before analysis. Successive laser pulses can be used to preferentially desorb material from the particle surface. Manual positioning of the particle under the beam makes the technique labor intensive. Quantitative determination of single compounds is limited by the reproducibility of the ion formation mechanisms and positioning of the beam.

The elemental composition of individual particles is also determined with transmission or scanning electron microscope (TEM, SEM) and X-ray and/or electron energy loss spectroscopy. EM techniques boast lower size resolution which is an order of magnitude better than other techniques. Particles are collected onto a substrate material of low atomic number, to minimize spectral and absorption interference from the substrate. Elemental analysis of inorganic salts such as sea-salt and ammonium sulfate can be performed for particles as small as 0.05 μm in diameter. Smaller particles containing heavier elements such as iron yield higher X-ray intensities and therefore are more easily detected. This technique offers the ability to observe and analyze small inclusions within a heterogeneous particle. Semi-quantitative analysis can be achieved with the use of laboratory generated particle standards of similar composition (McInnes et al., 1994). The precision of the technique is $\pm 10\%$ of the signal under ideal conditions for particles of the same composition and size. Differences in the net X-ray counts between same sized-particles is due to the difficulty of manually reproducing the beam conditions each time. High vacuum conditions in the EM make the analysis of volatile components, such as water or nitric acid, impossible. Light element detectors are used for the detection of the elements C, N, and O but at reduced sensitivities. Distinction between organic and graphic carbon is possible because graphic particles have a characteristic morphology (Sheridan et al., 1992). Molecular information can be obtained with chemical spot

tests for species such as NO_3^-, SO_4^{2-}, and NH_4^+ (Bigg et al., 1974; Weisweiler and Schwarz, 1988) with multiple reagent films used to simultaneously identify individual particle mixtures (Qian et al., 1991).

Ambient measurements of the number of sodium-containing particles can be made with a flame photometer and atomic emission spectroscopy (Radke, 1968). Aerosol particles are atomized in a high temperature flame causing metallic elements in the particle to evaporate and causing the electrons of the gas phase ions to be excited from ground state into higher energy orbitals. Upon relaxation the electrons lose energy in a characteristic manner resulting in an emission spectra, used to identify the elements of interest. Quantitative estimates of the number of atoms per particle (in this case, sodium) can be made. The lower size resolution for detection of sodium particles was reported at 0.3 μm, but could be improved significantly with modern technology.

A tandem differential mobility analyzer, TDMA, coupled with an aerosol conditioner can be used to sort aerosol particles based on their individual properties (Rader and McMurry, 1986). Measurements of the hygroscopic growth and volatility of aerosol particles corresponding to a narrow diameter range have been made (McMurry et. al., 1996; Covert and Heintzenberg, 1993; McMurry and Stolzenburg, 1989). Monodisperse aerosol particles are selected with the first differential mobility analyzer, DMA1, and the number concentration is measured with a condensation nucleus counter, CNC. The particles are then exposed to a controlled relative humidity, RH, or elevated temperature in the conditioner. The particle size may change in response to conditioning, dependent on its chemical composition. Upon exiting the conditioner, the changes in size of the aerosol particles is measured as a spectrum of growth or evaporation with a second DMA operated in scanning mode. The initial size, and resulting size distribution measured after conditioning are compared to evaluate the response of the aerosol to conditioning. The relative number of hygroscopic with respect to non-hygroscopic (or volatile with respect to non-volatile) particles as well as the relative amount of hygroscopic vs. insoluble material in the particles can be determined from the spectra. Similar determinations can be made with respect to volatility. Aerosol growth factors can be determined for a RH up to 95% to predict aerosol behavior in clouds or fogs. The TDMA sorts particles according to gross (but atmospherically relevant) integral properties, such as high or low hygroscopic growth factors or volatile mass fractions. While the results are reported for a population of particles, the sorting is done according to individual particle properties. The specific chemical composition of the particles for each mode can be determined by interfacing the system with analytical techniques previously mentioned.

1.2. Characteristics of the remote marine aerosol

The number size distribution of the submicrometer aerosol from the Pacific Marine Boundary Layer (MBL) is typically bimodal. As an example, measurements from the central Pacific in the springtime show a nuclei mode centered at 0.04 to 0.05 μm geometric mean diameter (gmd) and an accumulation mode located at 0.25 μm gmd for total aerosol number concentrations of 200 to 460 cm^{-3} (Quinn et al., 1993). An additional supermicrometer mode contributes a significant and variable portion to the total aerosol mass and surface area, although its number concentration is often less than a few particles cm^{-3}. Particles in the nuclei mode generally result from gas to particle conversion mechanisms, which occur in the marine boundary layer both in and out of clouds (Hegg et al., 1990; Covert et al., 1992; Hoppel et al., 1994). Nuclei mode particles contribute a significant and variable portion to the total number concentration, and are the nuclei of (and a major chemical input to) the accumulation mode. Accumulation mode particles result from the condensation of low volatility vapors, such as sulfuric acid and organics, onto pre-existing nuclei particles, by the uptake and reaction with gases such as SO_2 in the presence of water (cloud droplets) and by the coagulation of nuclei mode particles at high number concentrations. Sea-salt particles are also present in this size range and serve as reaction sites for sulfate conversion.

Particles in the accumulation mode whether from condensation or production at the sea surface represent a significant fraction of the total aerosol number and mass concentration. The number, size, and chemistry of these particles determines their effect on atmospheric properties, e.g., visibil-

ity, aerosol radiative forcing, and the number of cloud condensation nuclei. Lifetimes for these particles are relatively long when compared with the coarse mode aerosol, and the mass scattering efficiency (a dimensionless parameter used to estimate the size dependent contribution to the aerosol light scattering) is high. These factors collectively cause both the aerosol light scattering and number of CCN to be dependent on the number concentration and chemistry of the accumulation mode aerosol. The chemical heterogeneity of accumulation mode particles is dependent on the aerosol formation and transformation process. Chemical and morphological analysis of individual particles is needed, along with size selective bulk analysis, to understand such processes.

1.3. Approach

The elemental composition of homogeneous and heterogeneous aerosol particles above 0.05 μm diameter can be determined with analytical electron microscopy. It is possible to classify aerosol particles from the remote MBL into a few common groups based on their elemental spectra. However, in order to accurately determine the relative number concentration of each particle type, the aerosol collection and analysis must be representative of the population of particles in any mode of the number size distribution. To satisfy these requirements, ambient aerosol particles were collected onto TEM grids using a low pressure cascade impactor able to efficiently collect particles greater than 0.06 μm. Submicrometer particles were sampled collectively onto the same grid substrate, while supermicrometer aerosol particles were sampled with a separate impactor stage. The flow geometry of the impactor causes particles of different size to impact with characteristic surface density profiles on the substrate. Larger particles impact with higher concentrations near the center of the impaction jet, while smaller particles are distributed with higher concentrations further from the center. Therefore particle analysis statistics are strongly dependent on the radial position (distance from the impaction center) during the very localized EM analysis. The region chosen for EM analysis will only represent particle collection efficiencies for that location. It is therefore necessary to scan the entire impaction area, or convert particle size distributions obtained from the EM analysis at a few fixed radial positions to distributions representative of the ambient aerosol. This can be accomplished when particle collection efficiencies are known as a function of particle size and radial position.

Sethi and John (1993) measured the concentration density (surface density) under a round impactor jet as a function of particle Stokes number, St, where $\sqrt{\text{Stokes}}$ is proportional to the particle diameter Dp. Their results were used to normalize particle distributions obtained from our analysis. The normalized distributions, were then compared with aerosol size distributions measured in-situ during the field experiments. Because the aerosol size distributions measured by the independent techniques agreed fairly well, the relative abundance of sea-salt, sulfate, and carbonaceous particles as determined by EM analysis was considered representative of the ambient concentration for the size range under consideration.

2. Methods

2.1. Aerosol collection

Aerosol samples from the Pacific MBL were collected with a low pressure impactor (PIXE Corp. International, Tallahassee FL) onto EM grids by procedures outlined in McInnes et al. (1994) for EM analysis of size and elemental composition. Sampling occurred on board the NOAA ship Surveyor during the Radiatively Important Trace Species (RITS) experiment in March, April, and May of 1993, while the ship was in transit between Punta Arenas, Chile and Seattle, WA. The cruise track of the ship from 67°S, 140°W to 54°N, 140°W is shown in Fig. 1. Ambient samples were collected daily from the top of a mast 18 m above the sea surface. Collection times were between 2 and 15 min at a flow rate of 1.3 liter min^{-1} for fine aerosol ($\leqslant$2.0 μm) and 30 to 90 min for coarse aerosol ($>$2.0 μm). The established criteria for aerosol collection included conditions when local winds were greater than 2 m s^{-1} and within 45° of the bow, and the aerosol number concentration was below 1000 cm^{-3}. Aerosol sampling was discontinued when winds speeds were in excess of 15 m s^{-1}.

Aerosol samples were also collected in April of 1993 at the University of Washington research

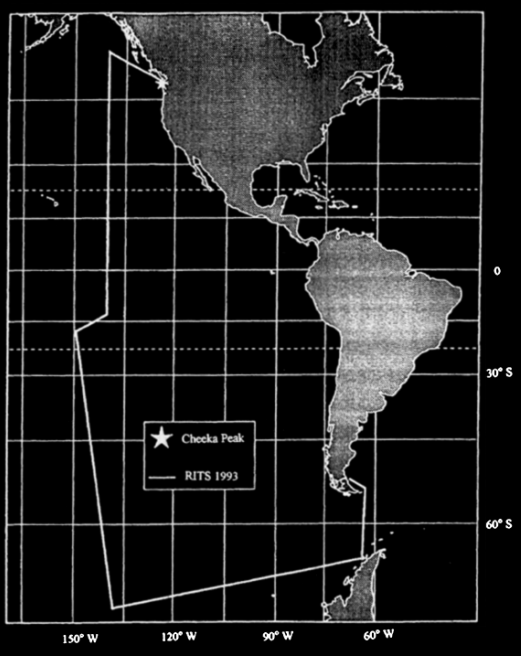

Fig. 1. Cruise track of the NOAA Surveyor during RITS-93. Relative location of the land-based sampling platform at Cheeka Peak, Washington is also shown.

station at Cheeka Peak, WA 48°N, 124°W during the Cloud and Aerosol Chemistry Experiment (CACHE-1). The research station is located at the top of a forested ridge, 480 m asl and 2 km inland of the Washington coast. Aerosol sampling was sector controlled for wind speed, wind direction, and total number concentration using the same criteria as in the RITS experiment. The impactor was installed at the outlet of a stack sampling 8 m above ground level. A total of 102 grid samples were collected for the coarse and fine aerosol fractions to represent the latitudinal variation encountered during the cruise, and the changing meteorological conditions encountered at Cheeka Peak.

In-situ aerosol number size distributions were measured continuously during both experiments corresponding to a dry size range of 0.02 to 9.6 μm. Aerosol size distributions for particles 0.02 to 0.6 μm were measured using a differential mobility analyzer (DMA, TSI model 3071, St. Paul, Minnesota) and condensation nucleus counter (TSI model 3760). Distributions were obtained over 17 separate size bins in approximately 15 minutes, or until the total number concentration measured for each bin was greater than 1000 cm^{-3} (Quinn et al., 1993). Size distributions for particles 0.6 to 9.6 μm were obtained with an aerodynamic particle sizer (APS, TSI model 3300).

2.2. *Individual particle analysis*

For calibration purposes, particles of ammonium sulfate, ammonium bisulfate, sodium chloride, and sea-salt were generated from 2% (by weight) solutions with a constant output atomizer (TSI model 3076). Solution droplets passed though a high capacity diffusion drier and charge neutralizer (^{85}Kr source) before entering the DMA analyzing region. Monodisperse aerosol particles were selected at 0.05, 0.20, and 0.50 μm (±10%) and impacted onto TEM grids. The impacted diameter, was compared with the diameter selected with the DMA for particles generated in the laboratory (Table 1). An example of the morphology of 0.50 μm sodium chloride particles is shown in Fig. 2.

Ambient aerosol particles were impacted onto SiO or carbon coated TEM grids. The morphology of the submicrometer aerosol particles from the remote Pacific atmosphere was spherical or near-spherical due to the hygroscopic nature of the particles coupled with the high RH during sampling. The diameter of the impacted particles upon drying was measured and calibrated against particles sized with the DMA (Liu and Piu, 1974). The impaction center of the grid was determined at low magnification and later used as a reference point to locate the region for analysis. Typically 5 to 7 regions (each of 39×39 μm^2 for 200 mesh, 100×100 μm^2 for 400 mesh grids) were selected for particle analysis. Between 50 and 100 particles were randomly selected for analysis to give Poisson counting uncertainties less than 10–15%. The elemental composition of each particle was

Table 1. *Relationship between impacted (D_{EM}) and DMA diameter*

Particle type	Morphology	D_{DMA}/D_{EM}
NaCl	cubic	1.2
sea-salt	cubic	1.0
NH_4HSO_4	spherical	0.9
$(NH_4)_2SO_4$	spherical	1.4

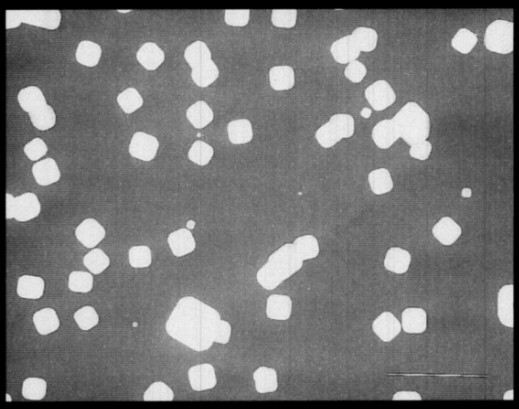

Fig. 2. Laboratory generated sodium chloride particles of 0.50 μm diameter. Larger particles represent doublets, and triplets with the same mass/charge ratio. Sizing bar: 2 μm.

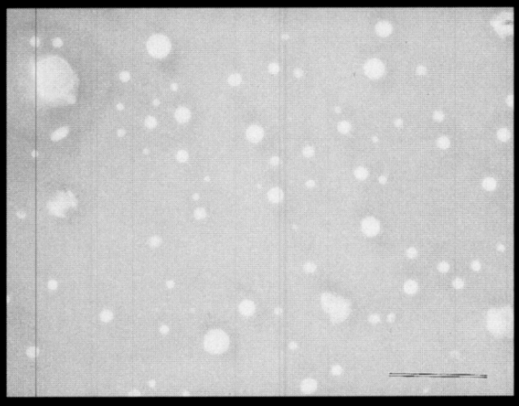

Fig. 3. Sulfate particles from the remote Pacific atmosphere showing a spherical morphology. Sizing bar: 2 μm.

determined with an X-ray detection system (KeVex Instruments, Inc., San Carlos, CA) able to identify elements of atomic number (Z) > 10, or Z > 5 using an UTW detector. Elemental spectra were acquired for 60 live seconds at a minimum count rate of 1000 counts s^{-1}. An accelerating voltage of 200 keV was used for the LaB_6 crystal at an operating current of 60 μA. With these instrumental conditions, no significant change in the elemental count rate occurred during analysis, implying no losses after initial vacuum desiccation. Particles were classified into groups based on their elemental spectra and particle morphology as summarized below. The most abundant particle types were sulfate, sea-salt, mineral, and carbonaceous aerosol.

2.3. *Particle types*

Sulfate aerosol. Aerosol particles which had a homogeneous spherical morphology and contained sulfur and oxygen were identified as sulfate particles (Fig. 3). Particles of ammonium sulfate, ammonium bisulfate, and sulfuric acid, all of which are known to exist in the remote MBL (Bigg, 1980), are included in this category. Although the elemental spectra for ammonium sulfate is indistinguishable from that of sulfuric acid, it is possible to make a coarse distinction between acidic sulfate, and neutralized sulfate based on particle morphology. Sulfate particles, acidic at the time of collection, show satellite rings surrounding a central spherical core after impaction (Ferek et al., 1983). For the purpose of this study, such a coarse distinction was sufficient.

Sea-salt aerosol. Sea-salt particles, including ones of heterogeneous composition (sea-salt particles containing additional sulfate material) were easily identified by their characteristic elemental spectra containing the elements Na, Cl, Mg, Ca, K, and S. Elemental ratios with respect to Na were constant for Mg, Ca, and K. However, sea-salt particles that have reacted with acidic species will have variable ratios of Cl and S. Sometimes, the amount of chloride remaining for fine mode sea-salt particles may be so low that it is no longer detectable in the particle (McInnes et al., 1994; Mouri and Okada, 1993). The amount of excess sulfate associated with chemically modified sea-salt particles can be determined by subtracting the amount of sea-salt sulfate; an amount which can be approximated by the SO_4^{2-}/Na^+ ratio in seawater.

Carbonaceous aerosol. Aerosol particles which contained carbon and oxygen at levels greater than 3 times the background signal of the substrate in a nearby particle-free region were identified as carbonaceous. Most of these particles did not contain any other identifiable elements and fell into two subcategories. Soot particles (graphic carbon) could be easily distinguished from other carbonaceous particles by a characteristic morphology of clusters of spheres (Fig. 4). Also the

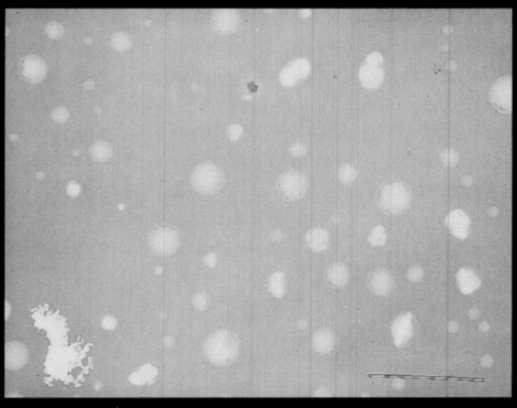

Fig. 4. The characteristic morphology of soot from aerosol collected during the CACHE-1 experiment. Sizing bar: 2 μm. (Soot particle, lower left.)

ratio of C/O was significantly lower for soot than for other carbonaceous aerosol. However the most abundant carbonaceous particles did not resemble soot, and had a spherical morphology (as shown in Fig. 5) and higher ratios of C/O. The composition is believed to be organic rather than that of an inorganic carbonate or soot, but no further chemical identification can be made. There were a significant number of particles which did not emit characteristic X-rays, above the substrate background which are also thought to be organic. Detector sensitivity for carbon is low and particles must contain about 30% of their total mass as carbon to be detected. Therefore aerosol particles containing carbon, but at levels below the instrumental detection limit, will not emit characteristic elemental spectra. Nitrogen-containing particles as well, for species such as ammonium nitrate, will not emit characteristic spectra due to the low detector sensitivity for nitrogen and the volatility of ammonium nitrate particles in the vacuum. However, homogeneous nitrate particles are not expected to contribute to the number of submicrometer particles in the MBL. Nitrate concentrations for submicrometer aerosol samples were much lower than sulfate concentrations for the RITS experiment (Quinn et al., 1995).

Mineral particles. A distinction was made between silica-rich mineral particles such as aluminosilicates and quartz, and particles which were rich in the following elements; K, Na, Ca, and Mg. Silicon minerals are derived from physical erosion of the continent and can be used as a tracer for air parcels which have passed over land. Aluminosilicate minerals contained variable quantities of Al, Si, K, Ca, Mg, and Fe while quartz particles contained only Si and O in their elemental spectra. Occasionally sulfur was identified in the mineral spectra suggesting these particles contained coagulated or condensed sulfate material from the atmosphere (Andreae et al., 1986). Particles containing K, Na, Ca, and/or Mg as the major elements were identified as metal carbonates and oxides. Many of these particles also contained measurable quantities of sulfur. Calcium sulfate particles were present in samples with an abundance of other mineral types, suggesting they were of continental, and not of marine origin.

Particles which were not be classified as either sea-salt, mineral, sulfate, or carbonaceous were grouped together. These particles represented less than 1% of the total number of particles analyzed and represented an even smaller fraction of the total aerosol number after normalization procedures. These particles were rich in iron and/or and titanium, and are thought to originate from an anthropogenic source.

2.4. Collection efficiencies of impacted particles in a well-defined region

With electron microscopy, it is not reasonable to analyze the elemental composition of every particle that is collected as a complete representation of the size distribution of a sample would demand. However, it is possible to determine the major features of the distribution by representative counting and normalization procedures, to estimate the geometric mean diameter of the aerosol modes (nuclei, accumulation, and coarse mode), the relative abundance of the major particle types for each mode, and the size distribution for each particle type. This was accomplished by analyzing the composition of particles over a pre-determined region of the grid where the size range of interest was represented, and relative particle collection efficiencies were known.

Particle collection efficiencies with respect to location under the jet of an impactor of similar geometry were obtained from the work of Sethi

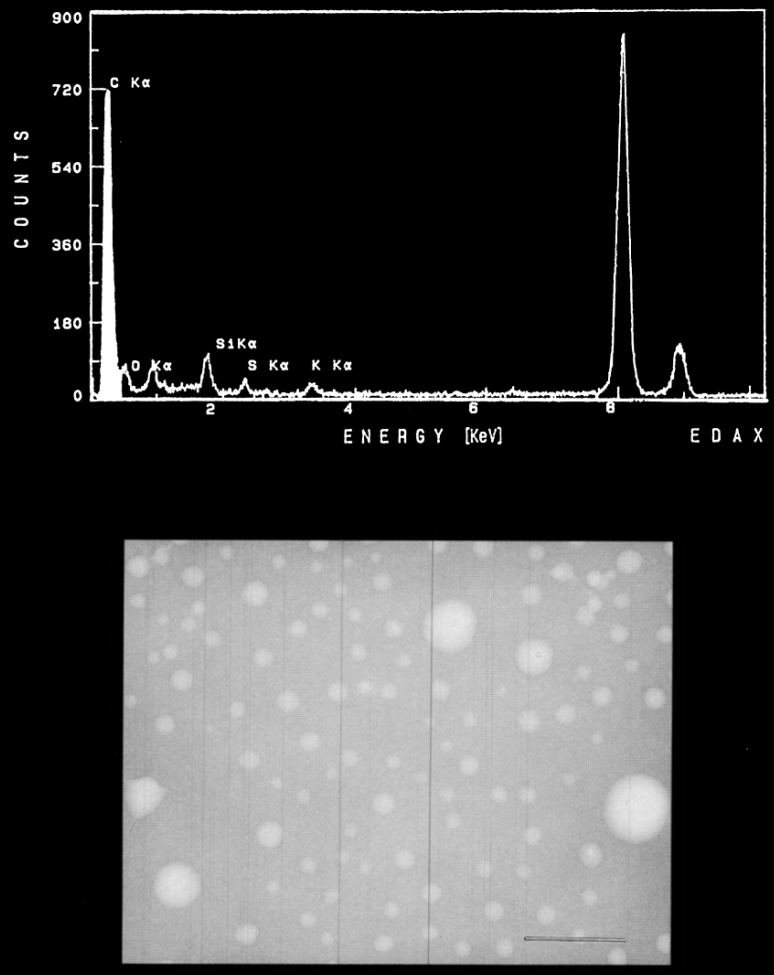

Fig. 5. Carbonaceous aerosol and X-ray spectra for particles collected during continentally influenced conditions at Cheeka Peak. The relative contribution from the grid substrate has been subtracted from the spectra. Sizing bar: 2 μm.

and John (1993), who measured surface concentrations (density) of monodisperse latex particles impacted from a circular jet. Using optical microscopy and automated image analysis, the authors found that the surface density reached a maximum at larger radial distances as a function of decreasing particle $\sqrt{\text{Stokes}}$ number. They established a relationship between the surface concentrations and radial position (measured from the center of the impaction jet) for $\sqrt{\text{Stokes}}$ number 1.6, 0.80, and 0.48 (Fig. 6). Larger particles were mostly confined to within the area of the impactor nozzle, with decreasing particle concentrations further from the jet. Smaller particles impacted at highest concentrations at increasing distance from the center.

Because the particle collection efficiencies are strongly dependent on the radial position, a specific region was pre-selected for analysis. Aerosol samples were collected on the last stage of the impactor using either the L1 or L2 stage corresponding to a D_{50} of 0.06, and 0.12 μm. The region chosen for analysis was located between 0.2 mm (r_1) to 0.4 mm (r_2) radial position. The area under the curve was integrated between 0.2 and 0.4 mm (Fig. 7) for each value of $\sqrt{\text{Stokes}}$ number in order to represent the total number of particles within this region. At the conditions of

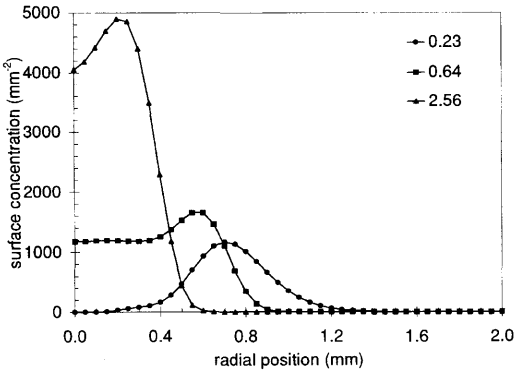

Fig. 6. Surface concentrations as a function of radial position measured from the impaction center. Reproduced using empirical relationships from Sethi and John (1993) for $\sqrt{\text{Stokes}}$ number 1.6, 0.80, and 0.48.

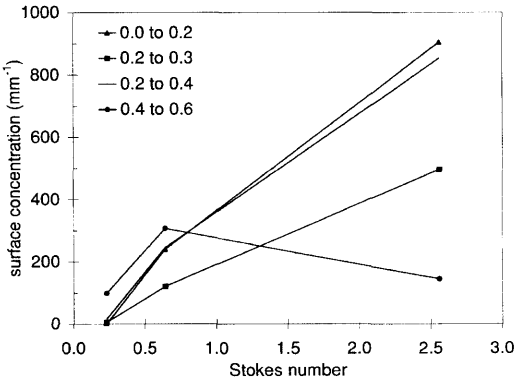

Fig. 7. Particle concentrations as a function of Stokes number integrated over the analysis regions 0.0 to 0.2 mm, 0.2 to 0.3 mm, 0.2 to 0.4 mm, and 0.4 to 0.6 mm.

sampling reported in Table 2 ammonium sulfate and sea-salt particles 0.05 to 0.5 μm diameter will have an equivalent Stokes number of 0.13 to 1.88 (impactor stage L2). It was necessary to extrapolate the results of Sethi and John (1993) for values falling outside of the reported range. Significant deviations however, are not expected to occur. Normalization factors (N, Table 3) were then calculated as $N = N_{St}/N_{ref}$ where N_{ref} was chosen as the number of particles at 0.2 μm, since they were found at the highest abundances. Normalized distributions were then compared to the in-situ distributions measured at the time of collection.

Table 2. *Ammonium sulfate and sea-salt particles: equivalent $\sqrt{Stokes}$ number*

Stage	Median diameter (μm)	Stokes number $\rho = 2.17$ g cm^{-3}	Stokes number $\rho = 1.77$ g cm^{-3}
LI	0.05	1.01	0.82
	0.10	2.02	1.65
	0.20	4.08	3.33
	0.30	6.18	5.04
	0.40	8.31	6.77
	0.50	10.47	8.54
	0.70	12.68	10.34
L2	0.05	0.16	0.13
	0.10	0.32	0.26
	0.20	0.66	0.54
	0.30	1.04	0.85
	0.40	1.44	1.18
	0.50	1.88	1.53
	0.70	2.35	1.92
	1.00	4.60	3.75

Table 3. *Normalization factors (N)*

Stokes number	N	Stokes number	N
0.23	0.09	1.65	2.98
0.26	0.18	1.88	3.37
0.32	0.35	1.92	3.44
0.54	1.00	2.02	3.60
0.64	1.29	2.33	4.12
0.66	1.35	2.35	4.16
0.82	1.60	2.56	4.51
0.85	1.65	2.85	4.99
1.01	1.91	3.33	5.80
1.04	1.96	3.75	6.50
1.18	2.20	4.08	7.05
1.44	2.63	4.60	7.92
1.53	2.78	—	—

3. Results

3.1. *Remote pacific*

In the MBL of the southern hemispheric Pacific, the relative number of sea-salt particles in the size range 0.1 to 1.0 μm diameter was fairly constant at 4 to 7% of the total number of particles in that range. The cumulative distribution of sub-μm sea-salt particles collected along the longitudinal transect of 140°W and 57°S, 42°S, 22°S, and 7°S latitude is shown in Fig. 8. There were two modes in the sea-salt number distribution having geomet-

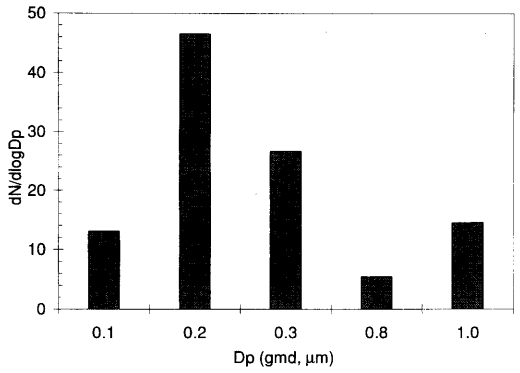

Fig. 8. Number distribution of sea-salt particles collected from the remote Pacific atmosphere over the size range 0.05 to 1.0 μm.

ric mean diameters of 0.2 μm and 0.6 μm, with a variable contribution from each mode for the samples examined. Sulfate particles, predominantly ammonium sulfate and acidic bisulfate, represented most of the accumulation mode number at 0.14 μm gmd. Sulfate particles were 96% of the total number for samples collected in the tropics at 22°S and 7°S. Airmass trajectories from this period indicate boundary layer residence times were at least 4 days long, originating over the open ocean to the south east. Samples collected in the midlatitudes from 57°S and 42°S also had a relatively large number of sulfate particles, representing 90% and 58% of the total number. During this period, boundary layer residence times were shorter, with the airmass originating from the Western S. Pacific. The total number concentration for these periods was also higher. Aerosol samples collected at 42° S had a significant number of carbonaceous particles representing 30% of the number, which are believed to be some type of condensed organic material. Submicrometer mineral particles contributed 4% to the total number during this period, suggesting the airmass had passed over land at some time and could potentially contain anthropogenic material. Aerosol particles from 57°S contained a small, but significant number of quartz minerals (1%) and carbonaceous particles (2%).

The agreement between aerosol number-size distributions collected in-situ and ones estimated from the EM analysis are shown in Figs. 9a–e. In-situ measurements show an accumulation mode centered at 0.09 μm gmd for 57°S and 42°S. Aerosol particles at 22°S and 7°S were somewhat larger with a mean diameter of 0.13 μm and 0.17 μm. Differences between the mean diameter estimated by EM and the in-situ analysis were 10% on average. The relative number of particles detected in each size bin with respect to the total number (0.10 to 0.50 μm) agreed fairly well for both the in-situ and EM analysis (Table 4), suggesting the EM analysis accurately represented the in-situ distribution over this size range.

In most cases, the number of coarse particles was underestimated by the EM technique as a result of the location within the impaction spot chosen for analysis. These particles however represent at the most 17% of the total number concentration (obtained from in-situ measurements). The coarse mode aerosol ($1.0 \leqslant Dp \leqslant 6.0$ μm) was predominantly sea-salt with a less abundant and variable fraction of mineral particles. Sea-salt particles made up 86 to 100% of the number concentration with mineral particles responsible for the remainder. Aluminosilicate particles had a mean diameter of 0.9 μm.

The relative number of sea-salt, sulfate, carbonaceous, and mineral particles at 52°N, 133°W, representing a midlatitude northern hemisphere location were compared with results from the southern hemisphere. Number concentrations were similar to those measured at 57°S and 42°S. The size distribution measured in-situ is shown in Fig. 9e. Along with it is a plot of the distribution obtained by EM analysis. The aerosol chemistry was again dominated by sulfate particles, representing 72% of the accumulation mode number concentration. Sea-salt particles were 13% of the total, which was noticeably higher than for samples examined from the southern hemisphere. Carbonaceous particles and minerals made up the remainder at 15% and 1% of the total.

3.2. *Marine/continental interface*

Aerosol samples from the northern hemisphere were also obtained from a land-based platform at Cheeka Peak (48°N, 124°W, 480 m asl) on the Washington coast. On average, aerosol number concentrations were higher than concentrations measured from the ship, positioned at the same latitude, suggesting there was a continental influence on the samples, despite proximity to the coast

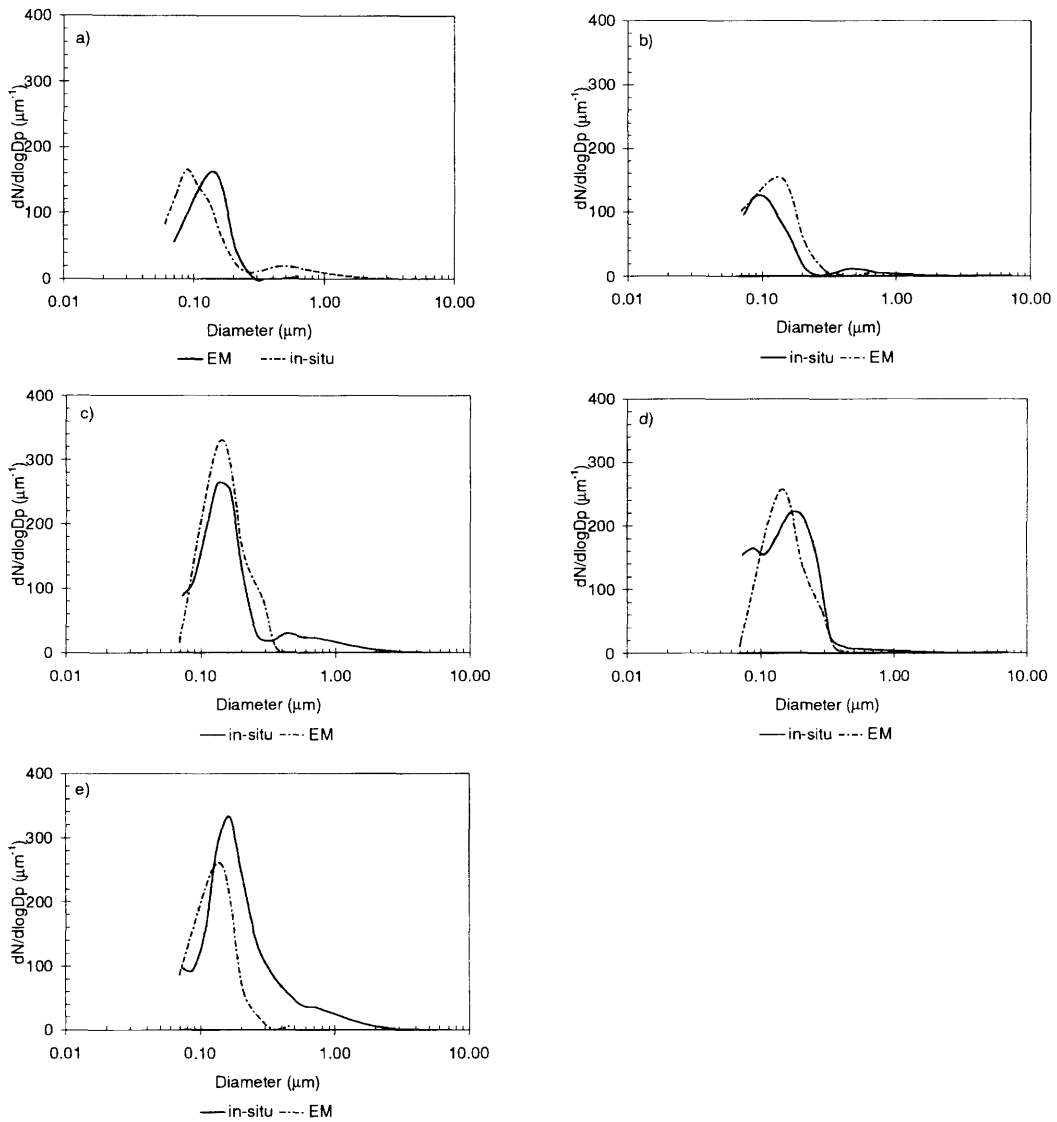

Fig. 9(a–e). Aerosol number size distributions measured in-situ during RITS-93. The corresponding size distributions obtained by EM analysis are also shown for the periods indicated.

	Lat, Long	Sampling period in-situ	EM
(a)	57°S, 144°W	93.972 to 0.979	93.974 to 0.977
(b)	42°S, 147°W	96.972 to 0.000	96.990 to 0.993
(c)	22°S, 147°W	100.965 to 0.979	100.969 to 0.971
(d)	7°S, 140°W	113.021 to 0.035	113.026 to 0.035
(e)	52°N, 133°W	125.875 to 0.889	125.878 to 0.880

and sector control for marine quadrant winds. Examples of the aerosol size distributions are shown in Figs. 10a, b, placed in order of increasing aerosol number concentration. Also shown are aerosol size distributions determined with EM analysis for the same periods.

Again, sulfate particles dominated the accumulation mode number concentration for Julian date

Table 4. *Comparative statistics of in-situ and EM distributions*

Figure	Diameter (μm)	N/N_{tot} in-situ	EM	Diameter (μm)	N/N_{tot} In-situ	EM
9a	0.10 to 0.14	0.63	0.78	0.17 to 0.21	0.21	0.21
9b		0.67	0.70		0.22	0.24
9c		0.49	0.57		0.41	0.27
9d		0.39	0.55		0.49	0.29
9e		0.35	0.77		0.46	0.18
10a		0.41	0.52		0.43	0.25
10b		0.23	0.26		0.32	0.33

N_{tot}: total number of particles measured between 0.10 and 0.50 μm.

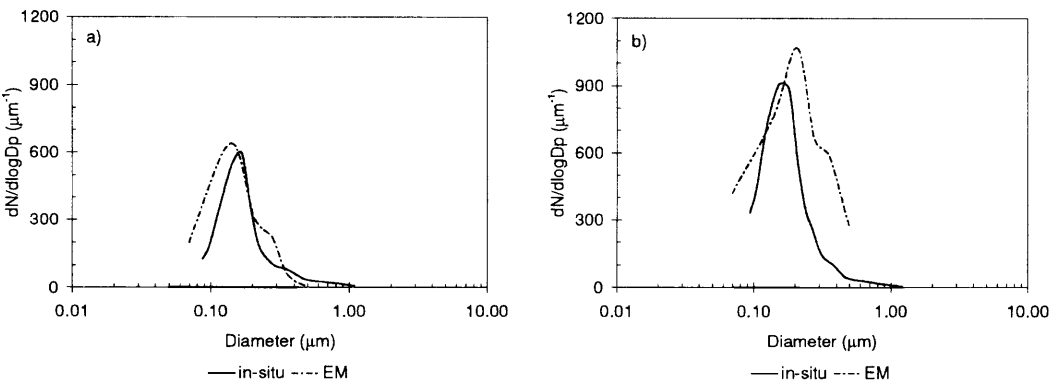

Fig. 10(a–b). Aerosol number size distributions measured in-situ during CACHE-1. Corresponding size distributions obtained by EM analysis are also shown for the periods indicated.

Figure	Location	Sampling Period in-situ	EM
(a)	Cheeka Peak	126.456 to 0.465	126.459 to 0.460
(b)	Cheeka Peak	134.590 to 0.597	134.594 to 0.595

(JD) 126 and 134 (May 6th, 14th 1993) representing 52% and 80% of the total. Sea-salt particles were 13 and 4% of the total number for these same periods. Carbonaceous particles were a significant fraction of the total for a sample collected on JD 126, but not on JD 134 (31% versus 2%). Mineral and calcium sulfate particles were identified in the sample on JD 126 (1% for both). Mineral particles were a significant fraction of a sample collected on JD 134, at 10% of the total number, mostly as aluminosilicates. The remaining fraction was identified as potassium sulfate particles.

During the experiment there were episodes with winds were from the south east, believed to originate from the metropolitan Puget Sound area and therefore representative of a polluted continental airmass. Aerosol number concentrations were highest during these periods, at concentrations around 3000 particles cm^{-3}. The aerosol composition was examined to determine the relative contribution of sulfate and carbonaceous particles to the total in an airmass which is known to be low in sulfur. The relative number concentration of sulfate particles reflected this with concentrations of only 7% of the total number in the accumulation mode. Carbonaceous particles were the major contributor at 89% of the total. Sea-salt particles were also present at 3% by number suggesting the air had some marine influence. Potassium sulfates were identified at a fraction of 1% of the number.

4. Conclusions

Measurements of the number of sulfate, carbonaceous, sea-salt, and mineral particles from

the remote Pacific atmosphere suggest that the aerosol number concentration is dominated by ammonium sulfate and acidic sulfate particles. Sea-salt particles are present in significant numbers in the submicrometric size range, at 4 to 13% of the total number. Carbonaceous and mineral particles did not significantly influence the total number concentration over the open ocean. However, when the airmass was influenced by the continent, the relative number of sulfate particles decreased with respect to the total, while the number of carbonaceous particles increased. Aerosol samples collected from the Pacific MBL indicate that carbonaceous particles (thought to be of organic composition) can be a significant contributor to the accumulation mode aerosol. Measurements from a coastal station in NW Washington suggest the carbonaceous aerosol is a significant contributor during polluted episodes and may outnumber the contribution from sulfate aerosol. Future efforts should address the chemistry, and hygroscopicity of the condensed organic species from natural and anthropogenic sources in order to evaluate its contribution to indirect aerosol radiative forcing.

5. Acknowledgements

The authors would like to acknowledge the National Center for Electron Microscopy (NCEM), Lawrence Berkeley Laboratories, at the University of California for sponsoring a Visiting Scientist Fellowship. Special thanks to Chuck Echer of NCEM for analytical assistance. A portion of this work was completed while the author was a Postdoctoral Fellow funded by the Cooperative Institute for Research in Environmental Sciences (CIRES) at the University of Colorado. This work was funded in part by the National Science Foundation Atmospheric Chemistry division grant #9311213. This paper is JISAO contribution number 355.

REFERENCES

Andreae, M. O., Charlson, R. J., Bruynseels, F., Storms, H., Van Grieken, R. and Maenhaut, W. 1986. Internal mixture of sea-salt, silicates, and excess sulfate in marine aerosols. *Science* **232**, 1620–1623.

Artaxo, P., Rabello, M. L. C., Maenhaut, W. and Van Grieken, R. 1992. Trace elements and individual particle analysis of atmospheric aerosols from the Antarctic peninsula. *Tellus* **44B**, 318–334.

Bigg, E. K. 1980. Comparison of aerosol at four baseline atmospheric monitoring stations. *J. Appl. Met.* **19**, 521–532.

Bigg, E. K., Ono, A. and Williams, J. A. 1974. Chemical tests for individual submicron aerosol particles. *Atmos. Environ.* **8**, 1–13.

Bruynseels, F. J. and Van Grieken, R. E. 1984. Laser microprobe mass spectrometric identification of sulfur species in single micrometer-size particles. *Anal. Chem.* **56**, 871–873.

Covert, D. S. and Heintzenberg, J. 1993. Size distributions and chemical properties of aerosol at Ny Ålesund, Svalbard. *Atmos. Environ.* **27A**, 2989–2997.

Covert, D. S., Kapustin, V. N., Quinn, P. K. and Bates, T. S. 1992. New particle formation in the marine boundary layer. *J. Geophys. Res.* **97**, 20581–20589.

Dierck, I., Michaud D., Wouters, L. and Van Grieken, R. 1992. Laser microprobe mass analysis of individual North Sea aerosol particles. *Environ. Sci. Techn.* **26**, 802–808.

Ferek, R. J., Lazrus, A. L. and Winchester, J. W. 1983. Electron microscopy of acidic aerosol collected over the northeastern united states. *Atmos. Environ.* **17**, 1545–1561.

Hegg, D. A., Radke, L. F. and Hobbs, P. V. 1990. Particle production associated with marine clouds. *J. Geophys. Res.* **95**, 13917–13926.

Heintzenberg, J. and Covert, D. S. 1990. On the distribution of physical and chemical particle properties in the atmospheric aerosol. *J. Atmos. Chem.* **10**, 383–397.

Hoppel, W. A., Frick, G. M., Fitzgerald, J. W. and Larson, R. E. 1994. Marine boundary layer measurements of new particle formation and the effects nonprecipitating clouds have on aerosol size distribution. *J. Geophys. Res.* **99**, 14443–14459.

Liu, B. Y. H. and Pui, D. Y. H. 1974. A submicron aerosol standard and the primary, absolute calibration of the condensation nuclei counter. *J. Colloid Interface Sci.* **47**, 155–171.

McInnes, L. M., Covert, D. S., Quinn, P. K. and Germani, M. S. 1994. Measurements of chloride depletion and sulfur enrichment in individual sea-salt particles collected from the remote marine boundary layer. *J. Geophys. Res.* **99**, 8257–8268.

McMurry, P. H. and Stolzenburg, M. R. 1989. On the sensitivity of particle size to relative humidity for Los Angeles aerosols. *Atmos. Environ.* **23**, 497–507.

McMurry, P. H., Litchy, M., Huang, P., Cai, X., Turpin, B. J., Dick, W. D. and Hanson, A. 1996. Elemental composition and morphology of individual particles separated by size and hygroscopicity with the TDMA. *Atmos. Environ.* **30**, 101–108.

Mouri, H. and Okada, K. 1993. Shattering and modification of sea-salt particles in the marine atmosphere. *Geophys. Res. Lett.* **20**, 49–52.

Murphy, D. M. and Thomson, D. S. 1995. Laser ionization mass spectrometry of single aerosol particles, *Aer. Sci. Techn.* **22**, 237–249.

Okada, K., Naruse, H., Tanaka, T., Nemoto, O., Iwasaka, Y., Wu, P., Ono, A., Duce, R. A., Uematsu, M., Merrill, J. T. and Arao, K. 1990. X-ray spectrometry of individual Asian dust-storm particles over the Japanese islands and the North Pacific ocean. *Atmos. Environ.* **24A**, 1369–1378.

Prather, K. A., Nordmeyer, T. and Salt, K. 1994. Real-time characterization of individual aerosol particles using time-of-flight mass spectrometry. *Anal. Chem.* **66**, 1403–1407.

Qian, G. W., Tanaka, H., Yamato, M. and Ishizaka, Y. 1991. Multiple thin film method for simultaneous detection of sulfate and nitrate ions in individual particles and its application to atmospheric aerosols. *J. Met. Society of Japan* **69**, 629–640.

Quinn, P. K., Covert, D. S., Bates, T. S., Kapustin, V. N., Ramsey-Bell, D. C. and McInnes, L. M. 1993. Dimethylsulfide/cloud condensation nuclei/climate system: Relevant size-resolved measurements of the chemical and physical properties of atmospheric aerosol particles. *J. Geophys. Res.* **98**, 10411–10427.

Quinn, P. K., Marshall, S. F., Bates, T. S., Covert, D. S. and Kapustin, V. N. 1995. Comparison of measured and calculated aerosol properties relevant to the direct radiative forcing of tropospheric sulfate aerosol on climate. *J. Geophys. Res.* **100**, 8977–8991.

Rader, D. J. and McMurry, P. H. 1986. Application of the tandem differential mobility analyzer to studies of droplet growth and evaporation. *J. Aerosol Sci.* **17**, 771–787.

Radke, L. R. 1968. *Automatic counting of cloud condensation nuclei. PhD Dissertation.* University of Washington, Seattle, Washington.

Sethi, V. and John, W. 1993. Particle impaction patterns from a circular jet. *Aeros. Sci. Techn.* **18**, 1–10.

Sheridan, P. J., Schnell, R. C., Hofmann, D. J., Harris, J. M. and Deshler, T. 1992. Electron microscope studies of aerosol layers with likely Kuwati origins over Laramie, Wyoming during spring 1991. *Geophys. Res. Lett.* **19**, 389–392.

Weisweiler, W. K. and Schwarz, B. U. 1988. A method for the qualitative and quantitative detection of individual NH_4^+-containing aerosols. *Atmos. Environ.* **22**, 755–762.

Wouters, L., Artaxo, P. and Van Grieken, R. 1990. Laser microprobe mass analysis of individual Antarctic aerosol particles. *Intern. J. Environ. Anal. Chem.* **38**, 427–438.